Electronic structure of organic superconductors κ-$(ET)_2Cu[N(CN)_2]Br$, κ-$(ET)_2Cu(NCS)_2$, and β-$(ET)_2I_3$ studied by photoelectron spectroscopy

Rong Liu, H. Ding, J. C. Campuzano, H. H. Wang, J. M. Williams, and K. D. Carlson
Materials Science and Chemistry Divisions, Argonne National Laboratory, 9700 South Cass Avenue, Argonne, Illinois 60439
(Received 5 January 1995)

Photoemission studies were carried out on three organic superconductors: κ-$(ET)_2Cu[N(CN)_2]Br$, κ-$(ET)_2Cu(NCS)_2$, and β-$(ET)_2I_3$. In all three compounds, we observe a valence band that extends from the Fermi level to approximately 22 eV below, showing many distinguishable features. A metallic Fermi edge is not observed in any of the three compounds. The orbital characteristics of some spectral features are deduced through variations in the excitation photon energy and observations of the relative intensity variations. For κ-$(ET)_2Cu[N(CN)_2]Br$ and β-$(ET)_2I_3$, comparisons were made between the measured spectra and the densities of states calculated by use of first-principles self-consistent methods. Some core-level spectra are presented.

I. INTRODUCTION

Organic superconductors have attracted increasing interest because of recent discoveries of new materials with higher T_c's.[1] The majority of organic superconductors, including those with the highest T_c's (>10 K), are charge-transfer salts derived from the electron-donor molecule BEDT-TTF, or ET [bis(ethylenedithio)-tetrathiafulvalene]. The ET-based organic superconductors have highly layered crystal structures consisting of alternating layers of ET molecules and inorganic anions. These compounds have many physical properties that are similar to those of the high-T_c copper oxide superconductors. For example, they both have highly anisotropic conductivities and short coherence lengths.

In this paper, we report photoemission studies of three ET-based organic superconductors: κ-$(ET)_2Cu[N(CN)_2]Br$ ($T_c=11.6$ K), κ-$(ET)_2Cu(NCS)_2$ ($T_c=10.4$ K), and β-$(ET)_2I_3$ ($T_c=1.4$ K). The 11.6 K transition temperature observed in κ-$(ET)_2Cu[N(CN)_2]Br$ is the highest among all ambient-pressure radical-cation-based organic superconductors reported to date. In our study, measurements were made on *in situ*-cleaved high-quality single crystals. The energy tunability of a synchrotron radiation source was exploited in an attempt to identify the orbital characteristics of spectral features. Additional information about the origin of the states can be obtained by comparing the spectra of three related compounds. These results provide a test for electronic-structure calculations.

To our knowledge, this is the first comprehensive photoemission study performed on this important group of materials. Itti *et al.*[2] reported valence-band and core-level spectra measured on as-grown or cleaved-in-air single crystals of κ-$(ET)_2Cu(NCS)_2$ using an Al K-edge x-ray source and He II radiation. It should be noted that the surfaces obtained by their surface preparation methods would inevitably have overlayers of adsorbed gas which are undesirable for photoemission study since photoemission is highly surface sensitive. Söderholm, Loppinet, and Schweitzer[3] reported a photoemission study of *in situ*-grown thin films of α-$(ET)_2I_3$, which is a semiconductor. Fermi-surface properties of κ-$(ET)_2Cu(NCS)_2$ and κ-$(ET)_2(NH)_4Hg(SCN)_4$ were studied by de Haas–van Alphen (dHvA) and Shubnikov–de Haas (SdH) experiments.[4–8] Kartsovnik *et al.* carried out Fermi-surface mapping on β-$(ET)_2IBr_2$ using angular magnetoresistance oscillations.[9] Recently, Jean *et al.* reported positron annihilation experiments on κ-$(ET)_2Cu[N(CN)_2]Br$.[10]

II. EXPERIMENTAL DETAILS

Photoemission experiments were carried out at the Argonne-Minnesota ERG-Seya beamline[11] at the Synchrotron Radiation Center, Stoughton, Wisconsin. Photoelectrons were collected by a 50-mm hemispherical analyzer mounted on a goniometer. The combined energy resolution (electron and photon) ranges from 50 to 150 meV for the spectra shown in this paper. The analyzer has an acceptance angle of 2°. Because the compounds under study have large crystallographic unit cells,[12] this angular resolution translates to a momentum window that is comparable to the Brillouin-zone dimensions. Thus the photoemission spectra should be viewed as angle-integrated results. The significant momentum integration is confirmed by the observation that the measured spectra do not show any noticeable variation, in either peak position or intensity, as the angle of the analyzer is changed. Single-crystal samples were grown by use of the electrocrystallization method.[13] They are flake shaped with a typical size of $1.5\times1.5\times0.2$ mm^3. Clean surfaces were obtained by cleaving in a vacuum better than 5×10^{-11} Torr. The cleavage surfaces contain the conducting a-c plane in κ-$(ET)_2Cu[N(CN)_2]Br$, the b-c plane in κ-$(ET)_2Cu(NCS)_2$, and the a-b plane in β-$(ET)_2I_3$.[12] Measurements were repeated on several samples for each compound and the results are reproducible.

III. RESULTS AND DISCUSSIONS

Shown in Fig. 1 is an energy distribution curve (EDC) measured on κ-$(ET)_2Cu[N(CN)_2]Br$ using $h\nu=24$ eV. Features labeled 1–8 at approximately −0.6, −1.6, −3.0, −3.8, −5.9, −7.3, −8.1, and −9.5 eV binding energies can be observed. We note that there are finite, although very small, emission intensities immediately below E_F. Shown in the inset are an EDC measured on the sample (lower curve) and an EDC measured on a platinum foil (upper curve) for the energy region close to E_F. Note that the emission intensity is near zero at exactly E_F in the spectrum of the sample. This spectral line shape is in contrast to a sharp Fermi edge usually observed in metallic systems where the Fermi level lies in the midpoint of the rising edge, as seen in the spectrum of a platinum foil. This unusual spectral behavior near E_F was discussed in detail in a previous paper.[14] The possibility of a surface artifact was considered but concluded to be unlikely. Electron-electron correlations and the excitation of phonons are the possible causes.

Shown in Fig. 2 are four EDC's measured on κ-$(ET)_2Cu[N(CN)_2]Br$ using photon energies between 40 and 160 eV. All spectra are normalized to the valence-band maximum. Because higher photon energies were used, three additional features labeled 9–11 at approximately −13.5, −16.5, and −19.2 eV binding energies can be observed.

It is evident that the relative intensities of various spectral features vary as the photon energy is changed. Most noticeably, the peak labeled 3 at approximately −3.0 eV binding energy becomes increasingly more intense when the photon energy is increased above 70 eV. Intensity variations can be consequences of two effects: matrix element effects and atomic photoexcitation cross section effects. Matrix element effects reflect excitations to non-free-electron-like final states in the solid. They are usually strong at low photon energies (e.g., $h\nu<40$ eV) and become less important at higher photon energies since the final states should be fairly free-electron like. The other effects are due to atomic photoexcitation cross sections. At low photon energies ($h\nu<50$ eV), the cross sections of the C $2p$ and S $2p$ states are much higher (by almost one order of magnitude) than those of C $2s$ and S $3s$.[15] At higher energies, the cross section of C $2s$ becomes dominant over C $2p$ and the cross section of S $3s$ becomes comparable to that of S $3p$. For the fairly high photon energies used in our experiment, it is reasonable to assume that most of the intensity variations are due to cross section effects. Based on the above information regarding atomic cross sections, the observation that the peak labeled 3 becomes more intense with increasing photon energy suggests that this state has dominant C $2s$ and/or S $3s$ character. The feature labeled A in the 70 eV spectrum also becomes stronger with increasing photon energy, indicating that it might also have dominant C $2s$ and/or S $3s$ character.

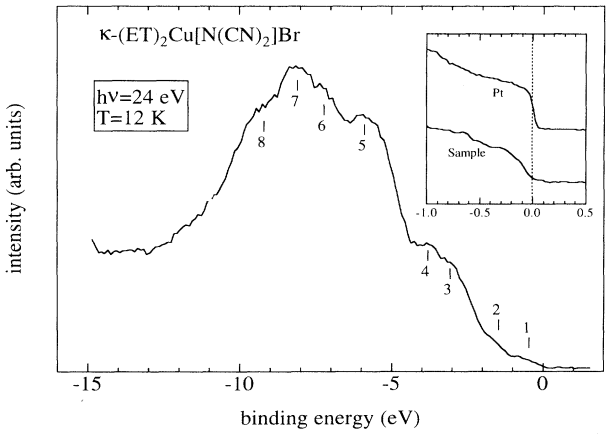

FIG. 1. An energy distribution curve (EDC) measured on κ-$(ET)_2Cu[N(CN)_2]Br$ using $h\nu=24$ eV. The inset shows an EDC measured on κ-$(ET)_2Cu[N(CN)_2]Br$ (lower curve) and an EDC measured on a platinum foil (upper curve) for the energy region near E_F.

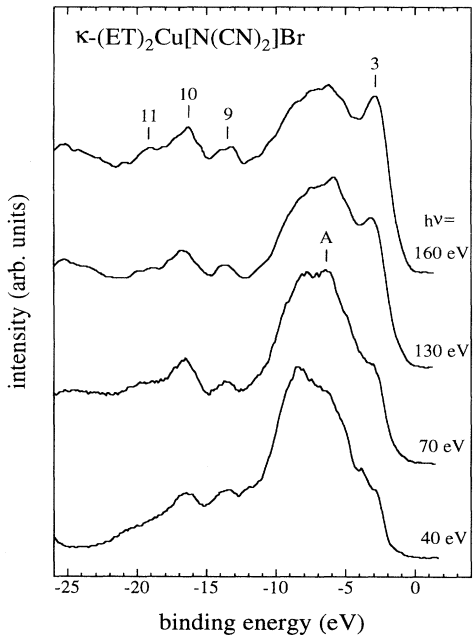

FIG. 2. EDC's measured on κ-$(ET)_2Cu[N(CN)_2]Br$ using several photon energies which are marked along each curve. All spectra are normalized to the valence-band maximum.

Shown in Fig. 3 are two superimposed EDC's measured with $h\nu=24$ and 40 eV. Both spectra are normalized to the valence-band maximum. Note that the emission intensities near E_F are significantly higher when using $h\nu=24$ eV than for $h\nu=40$ eV (see the inset). In particular, note that the 24 eV spectrum (solid line) shows a steplike emission onset near E_F whereas the 40 eV spectrum (dashed line) does not. This suggests that the states immediately below E_F have mainly C $2p$ and/or S $3p$ character.

Until recently, theoretical investigations of the electronic structure of the ET-based organic superconductors were limited to the semiempirical extended Hückel tight-binding method.[16] First-principles self-consistent calcula-

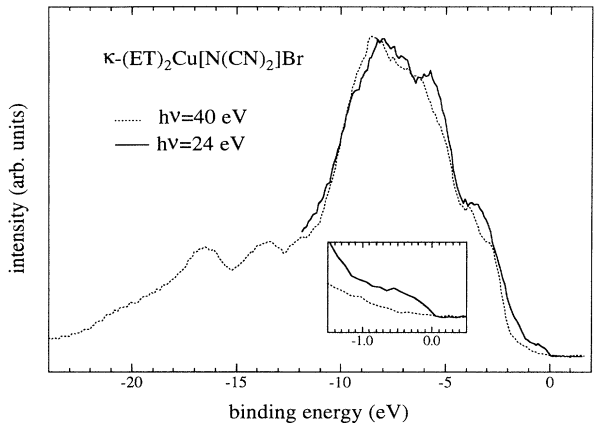

FIG. 3. Comparison of two EDC's measured on κ-$(ET)_2Cu[N(CN)_2]Br$ using $h\nu=40$ eV (dashed line) and $h\nu=24$ eV (solid line). Both spectra are normalized to the valence-band maximum. The inset magnifies the region near E_F.

tions are difficult because of the complex crystal structures that consist of large crystallographic unit cells. Ching *et al.* recently reported a self-consistent calculation for κ-$(ET)_2Cu[N(CN)_2]Br$ using the orthogonalized linear combinations of atomic orbitals (OLCAO) method.[17,18] Our measured valence-band spectra are compared with the calculated density of states broadened by a Gaussian function.[18] Correspondences can be found between most of the observed spectral features and the peaks in the calculated density of states. The partial agreement is encouraging given the complexity of the electronic structure.

In addition to κ-$(ET)_2Cu[N(CN)_2]Br$, we studied other two ET-based organic superconductors. Shown in Fig. 4 are EDC's measured on κ-$(ET)_2Cu(NCS)_2$ using photon

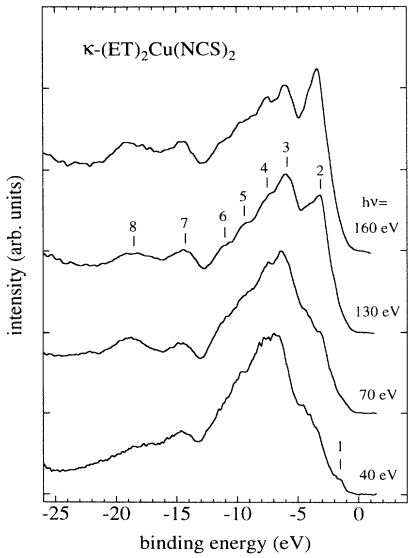

FIG. 4. EDC's measured on κ-$(ET)_2Cu(NCS)_2$ using several photon energies which are marked along each curve. All spectra are normalized to the valence-band maximum.

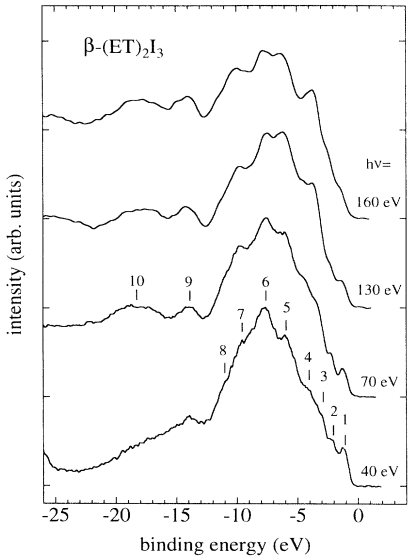

FIG. 5. EDC's measured on β-$(ET)_2I_3$ using several photon energies which are marked along each curve. All spectra are normalized to the valence-band maximum.

energies between 40 and 160 eV. All spectra are normalized to the valence-band maximum. We observe distinguishable features marked 1–8 at binding energies of approximately −1.5, −3.3, −6.0, −7.5, −9.3, −11.1, −14.3, and −18.5 eV. Note that the feature labeled 1 at −1.5 eV binding energy is more distinguishable in the 40 eV spectrum and becomes less discernible as the photon energy is increased. This trend suggests that this state has dominant C $2p$ and/or S $3p$ character. The feature labeled 2 at −3.3 eV binding energy becomes more intense as the photon energy is increased, indicating that it has dominant C $2s$ and/or S $3s$ character. We note that a metallic Fermi edge is also lacking in κ-$(ET)_2Cu(NCS)_2$.

Shown in Figs. 5 and 6 are EDC's measured on β-$(ET)_2I_3$ using several different photon energies. Features labeled 1–10 (Fig. 5) at approximately −1.2, −2.0, −3.0, −3.8, −6.0, −7.6, −9.6, −11.1, −14.0, and

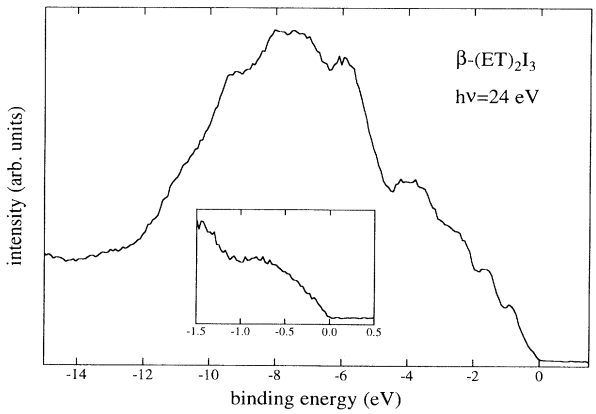

FIG. 6. An EDC measured on β-$(ET)_2I_3$ using $h\nu=24$ eV. The inset magnifies the region near E_F.

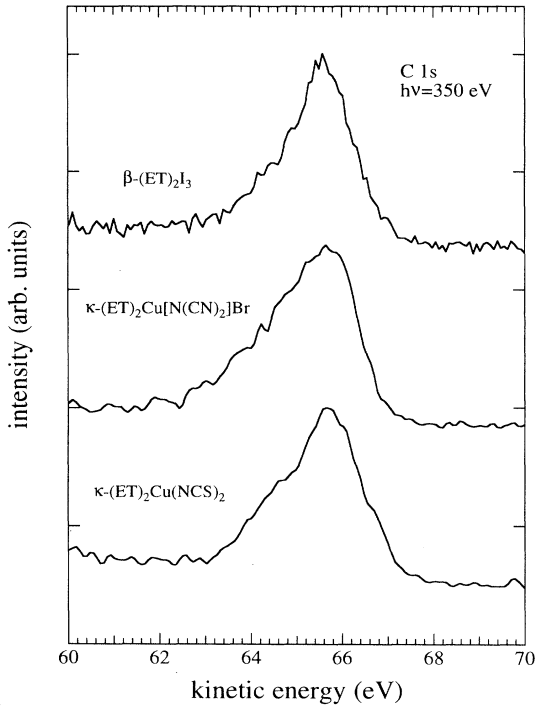

FIG. 7. C 1*s* core-level spectra measured on (from top to bottom) β-$(ET)_2I_3$, κ-$(ET)_2Cu[N(CN)_2]Br$, and κ-$(ET)_2Cu(NCS)_2$, using $h\nu=350$ eV.

-18.3 eV binding energies can be observed. The peak labeled 10 is rather broad indicating that it could be a superposition of two close peaks. Compared to the previous two compounds, the spectra of β-$(ET)_2I_3$ display more well-resolved peaks. For example, in the 40 and 70 eV spectra, the feature labeled 1 at -1.2 eV binding energy is rather narrow and acute. This feature becomes less intense as the photon energy is increased indicating that it has mainly C 2*p* and/or S 3*p* character. Other features also show rather dramatic intensity variations with photon energy. Peaks labeled 4, 5, and 7 become more intense with increasing photon energy, indicating that they have mainly C 2*s* and/or S 3*s* character. As can be seen clearly in the inset of Fig. 6, no metallic Fermi edge is observed in β-$(ET)_2I_3$ either. We observed that features labeled 2, 3, 5, 6, 7, 8, and 9 were also reported by Söderholm, Loppinet, and Schweitzer at nearly the same energies in *c*-axis-oriented thin films of α-$(ET)_2I_3$.[3]

Benedek *et al.* performed a self-consistent electronic-structure calculation for β-$(ET)_2I_3$ by use of the pseudopotential plane-wave method.[19] For binding energies between -2 and -10 eV, there exist excellent correspondences between the observed spectral features and the peaks in the calculated density of states broadened by a Gaussian function. The Gaussian-broadened density of states displays a local minimum at E_F which suggests that β-$(ET)_2I_3$ might be a semimetal. This provides another possible explanation for the lack of a Fermi edge observed in this material.

To summarize, photoemission measurements were carried out on κ-$(ET)_2Cu[N(CN)_2]Br$, κ-$(ET)_2Cu(NCS)_2$, and

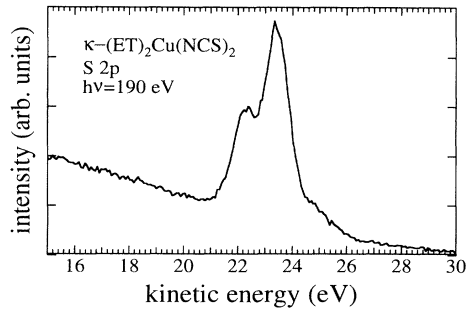

FIG. 8. S 2*p* core-level spectrum measured on κ-$(ET)_2Cu(NCS)_2$ using $h\nu=190$ eV.

β-$(ET)_2I_3$. In all three compounds, the valence-band spectra display an intense emission envelope that extends from E_F to approximately 12 eV below, showing many distinguishable features, and two to three well defined features between -12 and -22 eV binding energies. The latter features in the higher-binding-energy region appear similarly in the three compounds, suggesting that they may be primarily related to the common ET molecules. Söderholm, Loppinet, and Schweitzer came to the same conclusion based on the observation that these features also exist in iodine-deficient α-$(ET)_2I_3$ films.[3] In all three compounds, we observe a feature between -3 and -4 eV binding energy which becomes significantly more intense with increasing photon energy. This trend suggests dominant C 2*s* and/or S 3*s* character for this state. The consistent appearance of this feature in all three compounds suggests that it is mainly derived from the ET molecules. A metallic Fermi edge is not observed in any of the three compounds. For κ-$(ET)_2Cu[N(CN)_2]Br$ and β-$(ET)_2I_3$, partial agreements were found between the observed spectral features and the structures in the densities of states calculated by use of first-principles self-consistent methods.

We also measured C 1*s*, S 2*p*, Br 3*d*, and I 4*d* core-level spectra on these compounds. The C 1*s* spectra obtained from the three compounds have quite different line shapes (Fig. 7). Briefly, the C 1*s* spectrum of β-$(ET)_2I_3$ is slightly asymmetric and that of κ-$(ET)_2Cu[N(CN)_2]Br$ is strongly asymmetric with a tail on the higher-binding-energy side; that of κ-$(ET)_2Cu(NCS)_2$ shows distinguishable structures. These line shapes indicate multiple components and reflect the existence of chemically nonequivalent C sites in the structures. The differences in line shapes among the three compounds indicate that the number of nonequivalent C sites and their relative weights are different in each compound. The S 2*p* spectrum of κ-$(ET)_2Cu(NCS)_2$ shows a tail on the lower-binding-energy side in addition to the strong spin-orbit doublet (Fig. 8).

ACKNOWLEDGMENTS

We thank Dr. R. Benedek and Dr. W. Y. Ching for providing their calculation results prior to publication. This work is supported by the U.S. DOE under Contract No. W-31-109-ENG-38.

[1]For a recent review, see J. M. Williams, A. J. Schultz, U. Geiser, K. D. Carlson, A. M. Kini, H. H. Wang, W. K. Kwok, M. H. Whangbo, and J. E. Schirber, Science **252**, 1501 (1991); J. M. Williams, J. R. Ferraro, R. J. Thorn, K. D. Carlson, U. Geiser, H. H. Wang, A. M. Kini, and M. H. Whangbo, *Organic Superconductors* (Prentice-Hall, Englewood Cliffs, NJ, 1992).

[2]R. Itti, H. Mori, K. Ikeda, I. Hirabayashi, N. Koshizuka, and S. Tanaka, Physica C **185**, 2673 (1991); Mod. Phys. Lett. B **6**, 1785 (1992).

[3]S. Söderholm, B. Loppinet, and D. Schweitzer, Synth. Met. **62**, 187 (1994).

[4]J. Wosnitza, G. W. Crabtree, H. H. Wang, K. D. Carlson, M. D. Vashon, and J. M. Williams, Phys. Rev. Lett. **67**, 263 (1991).

[5]K. Oshima, T. Mori, H. Inokuchi, H. Urayama, H. Yamochi, and G. Saito, Phys. Rev. B **38**, 938 (1988).

[6]A. G. Swanson *et al.*, Solid State Commun. **73**, 353 (1990).

[7]M. V. Kartsovnik *et al.*, Sov. Phys. JETP **71**, 396 (1990).

[8]T. Sasaki *et al.*, Solid State Commun. **76**, 507 (1990).

[9]M. V. Kartsovnik *et al.*, J. Phys. (France) I **2**, 89 (1992).

[10]Y. C. Jean, Y. Lou, H. L. Yen, K. M. O'Broen, R. N. West, H. H. Wang, K. D. Carlson, and J. M. Williams, Physica C **221**, 399 (1994).

[11]C. G. Olson, Nucl. Instrum. Methods Phys. Res. Sect. A **266**, 205 (1988).

[12]For structural information, see Ref. 1.

[13]H. H. Wang, A. M. Kini, L. K. Montgomery, U. Geiser, K. D. Carlson, J. M. Williams, J. E. Thompson, D. M. Watkins, W. K. Kwok, U. Welp, and K. G. Vandervoort, Chem. Mater. **2**, 482 (1990).

[14]R. Liu, H. Ding, J. C. Campuzano, H. H. Wang, J. M. Williams, and K. D. Carlson, Phys. Rev. B **51**, 6155 (1995).

[15]J. J. Yeh and I. Lindau, At. Data Nucl. Data Tables **32**, 1 (1985).

[16]M. H. Whangbo *et al.*, in *Organic Superconductivity,* edited by V. Z. Kresin and W. L. Little (Plenum, New York, 1991), pp. 243–266.

[17]W. Y. Ching, Y. N. Xu, Y. C. Jean, and Y. Lou (unpublished).

[18]W. Y. Ching *et al.* (unpublished).

[19]R. Benedek *et al.* (unpublished).